
Journal of Aerospace Technology and Management
ISSN: 1984-9648
ISSN: 2175-9146
Departamento de Ciência e Tecnologia Aeroespacial

Keryk, Christopher; Sabatini, Roberto; Kourousis, Kyriakos; Gardi, Alessandro; Silva, Jose M.
An Innovative Structural Fatigue Monitoring Solution for General Aviation Aircraft
Journal of Aerospace Technology and Management, vol. 10, e0518, 2018
Departamento de Ciência e Tecnologia Aeroespacial

DOI: https://doi.org/10.5028/jatm.v10.779

Available in: https://www.redalyc.org/articulo.oa?id=309456744005

doi: 10.5028/jatm.v10.779 ORIGINAL PAPER

# An Innovative Structural Fatigue Monitoring Solution for General Aviation Aircraft

Christopher Keryk[1], Roberto Sabatini[1], Kyriakos Kourousis[1,2], Alessandro Gardi[1], Jose M. Silva[1]

Keryk C https://orcid.org/0000-0003-0479-9799
Sabatini R https://orcid.org/0000-0002-3399-2291
Kourousis K https://orcid.org/0000-0003-0861-4931
Gardi A https://orcid.org/0000-0003-4995-4166
Silva JM http://orcid.org/0000-0002-3176-5490

How to cite

Keryk C, Sabatini R, Kourousis K, Gardi A, Silva JN (2018) An Innovative Structural Fatigue Monitoring Solution for General Aviation Aircraft. J Aerosp Tecnol Manag, 10: e0518. doi: 10.5028/jatm.v10.779.

**ABSTRACT:** This article proposes a novel and effective solution for estimating fatigue life of General Aviation (GA) airframes using flight data produced by digital avionics systems, which are being installed or retrofitted into a growing number of GA aircraft. In the proposed implementation, a flight dynamics model is adopted to process the recorded flight data and to determine the dynamic loadings experienced by the aircraft. The equivalent loading cycles at fatigue-critical points of the primary structure are counted by means of statistical methods. For validation purposes, the developed approach is applied to flight data recorded by a fleet of Cessna 172S aircraft fitted with a Garmin G1000 integrated navigation and guidance system. Based on the initial experimental results and the developed uncertainty analysis, the proposed approach provides acceptable estimates of the residual fatigue life of the aircraft, thereby allowing a cost-effective and streamlined structural integrity monitoring solution. Future developments will address the possible adoption of the proposed method for unmanned aircraft structural health monitoring, also considering the accuracy enhancements achievable with advanced navigation and guidance architectures based on Global Navigation Satellite Systems (GNSS), Vision-Based Navigation (VBN) Sensors, Inertial Measurement Units (IMU) and Aircraft Dynamics Model (ADM) augmentation.

**KEYWORDS:** Aviation safety, Fatigue, General aviation, Cycle counting, Dynamic load, Manoeuvre identification, Structural integrity, Structural health, Vehicle health.

## INTRODUCTION

Aircraft operated and maintained beyond their intended design life will eventually incur primary structural failures unless structural health is properly monitored. The lack of vehicle health management solutions for a large variety of General Aviation (GA) aircraft and unmanned aircraft is therefore a growing issue, especially in countries where the mean fleet age is considerable. Affordable solutions that can meet the demands of GA operators and at the same time provide accurate information on the fatigue life of airframe components are therefore required. As an example, the Australian GA sector is largely composed of ageing aircraft operated and maintained well beyond their initial design lives, not in accordance with their intended Design Usage Spectrum (DUS) (Civil Aviation Safety Authority 2012). The mean age of GA fleet in Australia is 40 years, corresponding to more than twice their original design life (Civil Aviation Safety Authority 2012). Among other reasons, and despite their obsolescence, ageing GA are commonly retained in service in Australia as well as in several other countries due to their very competitive market prices,

**1.**RMIT University – School of Engineering – Melbourne, VIC – Australia. **2.**University of Limerick – School of Engineering – Limerick – Ireland.
**Correspondence author:** Alessandro Gardi | RMIT University – School of Engineering | PO Box 2471 | Bundoora, VIC 3083, Australia | Email: alessandro.gardi@rmit.edu.au
**Received:** Sep. 01, 2016 | **Accepted:** May 29, 2017
**Section Editor:** Valder Steffen Jr

limited devaluation, and very extensive and cost-efficient Maintenance, Repair and Overhaul (MRO) market. Analogously, a primary advantage of Unmanned Aircraft (UA) is their cost-effectiveness. Vehicle Health Management (VHM) is essential for avoiding critical structural failures, and its benefits in terms of safety are furthermore vital in the aviation domain, as structural failures are more likely to result in loss of life. Commercial and military aircraft operators invest heavily in VHM, with strict Aircraft Structural Integrity Management Plans (ASIMP) designed to assess the impact of the aircraft's operation on structural health. The GA sector however largely fails to monitor usage and track the 'structural lives' of their aircraft (Kourousis 2013). This is partially due to the considerable fatigue life considered in the design phase of the primary structures, and relatively smaller loads experienced compared to other aircraft types. In particular, adequate Margins of Safety (MS) inherent to the design are usually responsible for keeping the number of accidents related to structural health to a minimum. Notwithstanding, aircraft servicing performed according to the original design maintenance plan of most GA aircraft does not prevent fatigue failures that might occur once the aircraft exceeds its original design life, therefore continued use will degrade structural integrity and eventually lead to failure (Kourousis 2013; Molent and Aktepe 2000; Iyyer *et al.* 2008). Similarly to the GA sector, the UA sector also largely lacks dependable strategies for structural health monitoring. As the total number of flying UA and the number of their applications grow steadily, it will become critical to monitor their structural health to assess the safety of their operation.

Fatigue is one of the foremost structural health degradation issues in ageing airframes (Wahab and Paramonov 2010). Methods have been developed for measuring in-flight loads (Olkiewicz *et al.* 1994) and calculating structural fatigue in GA structures through a probabilistic safe life approach (Iyyer *et al.* 2008; Ocampo *et al.* 2010). The Palmgren-Miner damage model and other similar probabilistic approaches focus on calculating an informed damage index for the fatigue estimation based upon flight cycles. The theoretical behaviour of these models is often dissimilar to the statistical evidence due to the significant variety of loading configurations. Research and development has been performed on accelerometer-based fatigue-meters (Cicero *et al.* 2001; Zeiler *et al.* 2001; Marczi *et al.* 2004) which monitor flight loads and display a predicted residual fatigue life for the airframe. Units such as the one shown in Fig. 1 can be installed in the proximity of the Centre of Gravity (CG) of the aircraft to estimate the cumulative fatigue damage at critical locations. The retail prices of these dedicated Structural Health Monitoring (SHM) units can be considerable, especially in comparison with the residual value of ageing aircraft. Consequently, the adoption of these technologies has been low (Civil Aviation Safety Authority 2012), but uptake could be improved with the development of cheaper alternatives.

**Figure 1.** TK Elektronic structural life monitoring unit TL-5824.

This paper presents an innovative SHM method specifically developed for the GA and UA sectors. The proposed SHM approach is based on the analysis of raw flight data retrieved by low-cost navigation and guidance systems of GA aircraft and UA, therefore it does not require dedicated equipment. The paper describes the software algorithms for the post-processing of these data to determine the loads at fatigue-critical locations in the primary structure, and estimate the residual fatigue life of the airframe. As an initial verification, the method was applied to a fleet of Cessna 172 Skyhawk aircraft operated by RMIT University Flight Training at the Royal Australian Air Force (RAAF) Williams airbase in Point Cook (Victoria), which are fitted with Garmin G1000 digital flight instruments. The article includes an uncertainty analysis to evaluate the accuracy of the method. The low error figures obtained support the validity of the proposed SHM approach for estimating the residual fatigue-life of GA and UA aircraft.

## PROPOSED SHM METHOD

SHM solutions requiring the retrofit of expensive dedicated equipment will fail to meet the expectations of GA and UA communities. An SHM approach based on low-complexity and low-cost cumulative fatigue assessment methods would hence prove more suitable for cost-sensitive sectors, including the Australian GA and UA. Given that most GA aircraft are not equipped with strain gauges it is therefore necessary to resort to any data available from on-board equipment to determine the dynamic loads endured by the structure. Furthermore, in order to be accessible to the widest possible range of GA aircraft and UA, and consequently successful in minimizing the number of unsafe aircraft flying, the SHM system must be cost-effective and easily deployable within the existing GA and UA fleet, and consequently should not impose additional equipment, structural modifications or certification requirements (McColl and Iyyer 2008). Therefore, an exploitation of the installed avionics offers a promising low-cost alternative. The SHM system must accommodate aircraft that are not equipped with high accuracy multi-sensor navigation systems or strain gauges. A growing number of GA aircraft is retrofitted with modern commercial-of-the-shelf digital avionics capable of recording flight data for post-processing. Computing aircraft loadings from recorded flight data makes dedicated fatigue monitoring units unnecessary, thereby reducing the costs associated with SHM and easing its adoption. Determining cumulative damage without a dedicated load cycles measuring unit also allows for retrospective damage analysis of the structure where historical log files are available. This process will enable a streamlined implementation for GA fatigue management, especially in new aircraft. The SHM system must be dependable to accurately assess structural health and consequently supersede the manufacturer's design life. In particular, the method must be accurate, repeatable, efficient, and based on readily available data. Subcomponents and systems can be overhauled or refurbished, but in the case of the primary structure of an aircraft (*e.g.* the wing), the cost would be prohibitive for most GA operators considering the residual value of an ageing aircraft, so residual fatigue life estimations must be accurate to minimize waste. The SHM system must also include data quality verification to ensure the integrity of the results (Aktepe and Molent 1999). In particular, it is expected that the flight data available from the avionics existing on-board will not necessarily be complete and may include noise and spurious readings, so a flexible solution based on expert data processing has the best chance of success. The low-cost SHM process for GA and UA proposed here is presented in Fig. 2 and was developed capturing the aforementioned requirements and the considerations presented in McColl and Iyyer (2008).

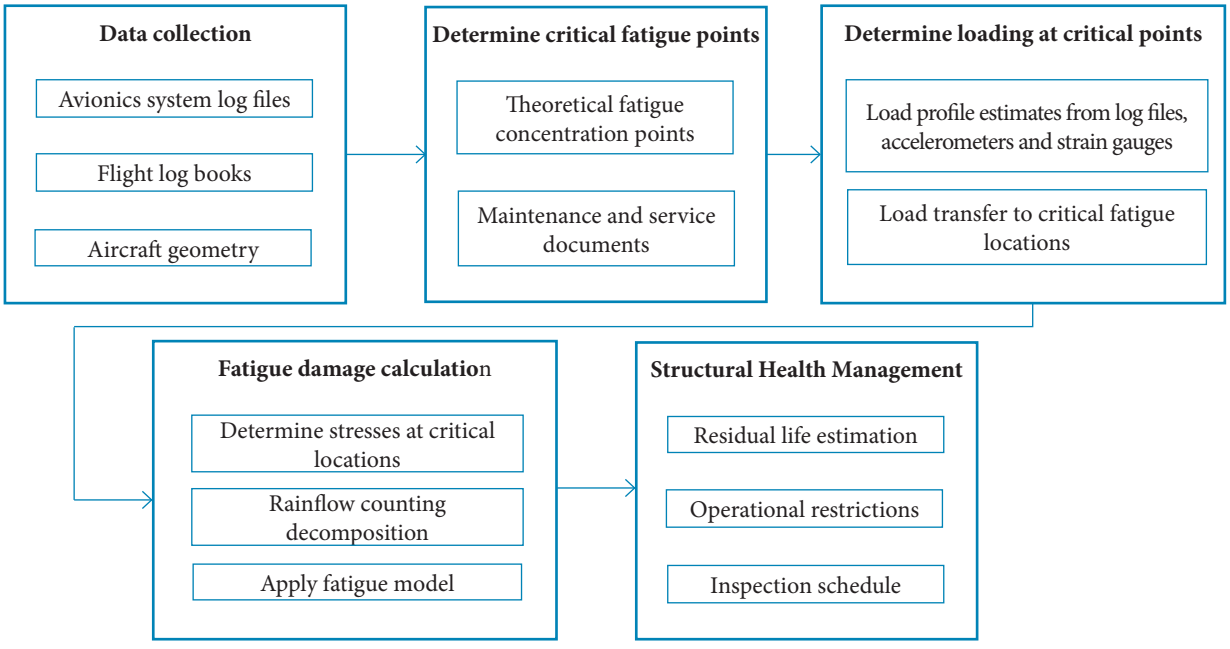


**Figure 2.** Proposed structural health management process.

In the proposed approach, critical structural locations are identified based on their susceptibility to fatigue damage and their safety-critical role in the primary structure (Swanton and Walker 1997). These locations vary between aircraft makes and models due to differences in design, but for conventional aircraft configurations there are some common locations. For instance, in conventional GA aircraft, fatigue-critical locations include attachment points, rivet lines, spar booms, etc. (Marczi 2004). Our investigation focusses on the Cessna 172, whose fatigue-critical structural locations were identified through a survey of the released Supplementary Inspection Documents (SID) and published data related to other similar aircraft. As depicted in Fig.3, the identified points include the wing attachments, wing struts and horizontal and vertical tail attachment points.

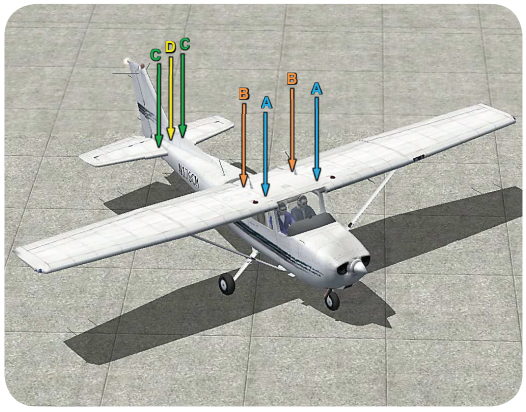


A: Front wing attachments
B: Rear wing attachments
C: Horizontal stabilizer attachment
D: Vertical stabilizer attachement

**Figure 3.** Cessna 172 primary critical structure fatigue locations.

To determine the cumulative fatigue damage and structural health, the measured loading spectrum is related to the stresses at the critical points by use of transfer functions. These transfer functions are either supplied by the manufacturer or formulated a posteriori through two methods: empirical strain gauge based stress correlations or Finite Element (FE) analysis. In the first method, strain gauges are attached to the fatigue-critical locations and the stresses and g-loadings are logged during flight testing campaigns to experimentally determine the empirical correlation parameters. A test bed aircraft is required as the installation of strain gauges may be impractical and may affect certification. The second method involves performing FE analysis to determine the correlation coefficients. Once developed, FE models can be reused with different load configurations whenever deemed appropriate (Marczi 2004). The FE-based approach proves adequate in most circumstances when it is not possible to perform actual flight testing to obtain experimental correlations. Loads are converted into stresses by accurately introducing component geometries and material properties, which for ageing GA aircraft are commonly available in the public domain. Similarly, it is necessary to obtain or produce Stress-Life (S-N) curves of the critical components to perform the fatigue calculation. This information is readily available in the public domain for popular GA aircraft, such as the Cessna 172. Alternatively, published S-N curves for the specific material of the component can be employed. The stress history retrieved from the navigation data is decomposed through a cycle counting method. In order to estimate the fatigue life of a simple periodic loading, counting methods are unnecessary as cycles can easily be determined. Random variable amplitude loadings though cannot be simply assessed by counting maxima and minima cycles and must be analysed with a cycle counting method, such as rainflow analysis. In particular, rainflow analysis allows decomposing a complex variable amplitude load history and converting it to equivalent number of constant amplitude stress cycles and half-cycles. Rainflow counting involves combining the load history, and particularly the local maxima and minima (inversion) points to compose equivalent load cycles which can be compared with the number of cycles to failure for the given magnitude to determine cumulative fatigue damage. The rainflow counting is based on the principle that a loaded material will load and unload between the maximum and minimum points identical to a scenario with no intermediate loadings (Musallam and Johnson 2012) as depicted in Fig. 4, where  represents the strain,  represents the stress and $t$ stands for time. Each closed loop has a mean strain range and mean stress that can be compared with a constant amplitude cycle. For example, as the section deforms from $A$ to $B$ it follows a path given by its cyclic stress-strain curve. At point $B$ the loading is reversed and the

section unloads elastically to point *C* before reversing again and loading up to point *B*. Beyond point *B* the section loads to *D* according to its stress-strain properties as though the phase *B*-*C*-*B* never occurred. This assumption is valid as long as the cycle is performed within the limits of the elastic regime of the material. Stresses exceeding the elastic regime are not considered in our approach, as their occurrence might expose the vehicle to non-fatigue related failure modes and, based on the current standards, void the airworthiness of the aircraft altogether.

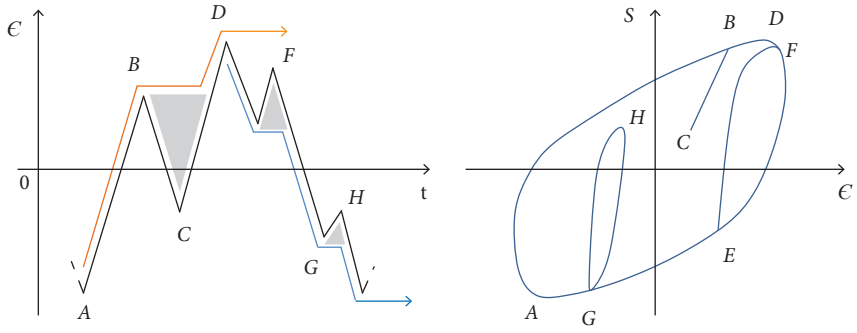


**Figure 4.** Stress-strain cycles. Adapted from Musallam and Johnson (2012).

Subsequently the cumulative fatigue is estimated based on the total cycle count using established methods such as the Palmgren-Miner damage law (Dowling 1988; Boller and Buderath 2007; Federal Aviation Authority 2005; Marczi 2004), crack growth (Molent *et al.* 2008; Zhuang *et al.* 2007) or probabilistic methods (Molent and Aktepe 2000; Ocampo *et al.* 2010; Xiang and Liu 2011). The Palmgren-Miner damage law is a linear fatigue damage theory that estimates cumulative fatigue damage at critical locations. The Palmgren-Miner damage law states that failure will occur when the damage index (*DI*) is equal to one, where the damage index is a summation of all cycles for each load ($n_i$) divided by the number of cycles to cause failure at that load ($N_i^f$). The residual life in flight hours ($T_{res}$) can be estimated using the time ($\tau$) taken to reach the current damage index, for instance using a linear approximation. This is expressed by the following equations:

$$DI = \sum \frac{n_i}{N_i^f} \; ; i = 1 \ldots s \tag{1}$$

$$T_{res} = (T_{des} - \tau)(1 - DI(\tau)) \tag{2}$$

where $T_{res}$ is the structural design life of the aircraft, either prescribed by the manufacturer or determined empirically from aircraft historical usage data. Equation 2 fulfils the following boundary conditions:

- $DI(0) = 0 : T_{res} = T_{des}$
- $DI(T_{des}) = 1 : T_{res} = 0$

The $DI(\tau)$ function can be determined and calibrated empirically (via the collection and analysis of aircraft historical usage data).

In order to determine the loadings undergone by the aircraft along the body axes based on the raw avionics log data, a 6-Degree-of-Freedom (6-DOF) flight dynamics model of the aircraft is adopted. The 6-DOF is a rigid body model that captures all translational and rotational dynamics and therefore accounts for the full set of loadings experienced by the aircraft. By means of analytical inversion, a 6-DOF model can be used to determine the forces and moments on the aircraft, provided that the required state variables, including velocities and rotations, are known. If some of the states are not available nor can be derived from the

dataset, it will be necessary to reconstruct the missing state by means of optimal estimation and/or to resort to a less accurate 3-DOF point-mass model. Considering the information available from the Garmin G1000 log files, a full 6-DOF rigid body model could be directly adopted. Thus, the loadings at the centre of gravity are determined based on the following analytical derivation. For further detail the reader may refer to Zipfel (2007). The standard Newton's equations for 6-DOF dynamics expressed in the aircraft body frame are:

$$a_X = \frac{\Sigma F_X}{M} = \dot{u} - rv + qw \tag{3}$$

$$a_Y = \frac{\Sigma F_Y}{M} = \dot{v} - pw + ru \tag{4}$$

$$a_Z = \frac{\Sigma F_Z}{M} = \dot{w} - qu + pv \tag{5}$$

where $\dot{u}, \dot{v}, \dot{w}$ are the velocities respectively along the $X, Y, Z$ axes of the body reference frame; $p, q, r$ are the angular velocities respectively around the $X, Y, Z$ axes of the body reference frame; $F_{X,Y,Z}$ is the force components respectively along the $X, Y, Z$ axes of the body reference frame; $a_{X,Y,Z}$ is the acceleration components respectively along the $X, Y, Z$ axes of the body reference frame; $M$ is the aircraft mass.

The angular velocities in the body reference frame ($p$, $q$, $r$) of Eqs. 3-5 can be expressed in terms of the Euler rotations of the aircraft as follows:

$$p = \dot{\varphi} - \dot{\psi} \sin\theta \tag{6}$$

$$q = \dot{\theta} \cos\varphi + \dot{\psi} \cos\theta \sin\varphi \tag{7}$$

$$r = \dot{\psi} \cos\theta \cos\varphi - \dot{\theta} \sin\varphi \tag{8}$$

where $\dot{\varphi}, \dot{\theta}, \dot{\psi}$ are the three Euler angles respectively defining aircraft's roll, pitch and yaw. On the other hand, the body frame velocities ($u$, $v$, $w$) of Eqs. 1-3 can be derived from the velocities along the inertial reference frame of choice, which in our case is the North-East-Down (NED). This can be achieved by applying the transformation matrix resulting from composing all the three Euler rotations. By abbreviating *sin* with *s* and *cos* with *c*, we may write the full transformation between the inertial frame and the body frame as:

$$\begin{bmatrix} u \\ v \\ w \end{bmatrix} = \begin{bmatrix} c\theta\, c\psi & c\theta\, s\psi & -s\theta \\ s\varphi\, s\theta\, c\psi & s\varphi\, s\theta\, s\psi + c\varphi\, c\psi & s\varphi\, c\theta \\ c\varphi\, s\theta\, c\psi & c\varphi\, s\theta\, s\psi - s\varphi\, c\psi & c\varphi\, c\theta \end{bmatrix} \begin{bmatrix} U \\ V \\ W \end{bmatrix} \tag{9}$$

where $U, V, W$ are the velocities in the North-East-Down (NED) reference frame. These velocities in the NED reference frame are in turn obtained from discrete positions as follows. A great circle arc segment is calculated between discrete geodetic positions recorded in the log files in terms of latitude $\varphi$ and longitude $\lambda$. The arc segment is divided by the time step, also recorded in the log files. The expressions for calculating the discrete velocities in the NED frame from the recorded data are therefore:

$$U_i = \frac{\Delta d_i}{\Delta t} = 2\, R\, arcsin\left(\sqrt{sin^2 \frac{\phi_{i+1} - \phi_{i-1}}{2}}\right) / \left(t_{i+1} - t_{i-1}\right) \tag{10}$$

$$V_i = \frac{\Delta d_i}{\Delta t} = 2\,R\,arcsin\left(\sqrt{\cos^2\phi_i \cdot sin^2\frac{\lambda_{i+1}-\lambda_{i-1}}{2}}\right) / (t_{i+1}-t_{i-1}) \tag{11}$$

$$W_i = \frac{h_{i+1}-h_{i-1}}{t_{i+1}-t_{i-1}} \tag{12}$$

where $U$, $V$, $W$ are the velocities in the North-East-Down (NED) reference frame; $d_i$ is the distance travelled measured on a great circle arc segment; λ is the geodetic longitude (recorded); $\phi$ is the geodetic latitude (recorded); $R$ is the Earth radius; $t$ is the time (recorded).

The accelerations in the inertial reference frame are also calculated through a discrete central differentiation similar to Eq. 12. These accelerations in the inertial frame are also transformed in the body frame and used for comparison to validate the algorithms.

## UNCERTAINTY ANALYSIS

An uncertainty analysis is performed to estimate the combined effects of the various contributing error sources affecting the model. Based on Eqs. 3-12, it is possible to apply the standard propagation of uncertainty theory to calculate the uncertainty in CG accelerations in body axes as a function of the uncertainty in the raw measurements. For arbitrary multivariate nonlinear functions such as the ones in the 6-DOF model of Eqs. 3-12, the propagation of uncertainty theory requires a multivariate Taylor polynomial expansion to the first order. Following this approach, the following expressions were developed:

$$\sigma_{a_X}^2 = \left(-\dot{U}s\theta c\psi - \dot{V}s\theta s\psi - \dot{W}c\theta\right)^2\sigma_\theta^2 + \left(-\dot{U}c\theta s\psi + \dot{V}c\theta c\psi\right)^2\sigma_\psi^2 + (c\theta c\psi)^2\sigma_{\dot{U}}^2 + (c\theta s\psi)^2\sigma_{\dot{V}}^2 + (-s\theta)^2\sigma_{\dot{W}}^2 \tag{13}$$

$$\sigma_{a_Y}^2 = \left(\dot{U}s\varphi c\theta c\psi + \dot{V}s\varphi c\theta s\psi - \dot{W}s\varphi s\theta\right)\sigma_\theta^2 + \left[\dot{U}(c\varphi s\theta c\psi + s\varphi s\psi) + \dot{V}(c\varphi s\theta s\psi - c\psi s\varphi) + \dot{W}c\varphi c\theta\right]^2\sigma_\varphi^2 + \tag{14}$$
$$+\left[\dot{U}(-s\varphi s\theta s\psi - c\varphi c\psi) + \dot{V}(s\varphi s\theta c\psi - s\psi c\varphi)\right]^2\sigma_\psi^2 + (s\varphi s\theta c\psi - c\varphi s\psi)^2\sigma_{\dot{U}}^2 + (s\varphi s\theta s\psi + c\psi c\varphi)^2\sigma_{\dot{V}}^2 + (s\varphi c\theta)^2\sigma_{\dot{W}}^2$$

$$\sigma_{a_Z}^2 = \left[\dot{U}(c\varphi c\theta c\psi + s\theta s\psi) + \dot{V}(c\theta c\varphi s\psi - c\theta c\psi) - \dot{W}c\varphi s\theta\right]^2\sigma_\theta^2 + \left(-\dot{U}s\theta s\varphi c\psi - \dot{V}s\theta s\varphi s\psi - \dot{W}s\varphi c\theta\right)^2\sigma_\varphi^2 + \tag{15}$$
$$+[U(-c\varphi s\theta s\psi + s\theta c\psi) + V(c\varphi s\theta c\psi + s\psi s\theta)]^2\sigma_\psi^2 + (c\varphi s\theta c\psi + s\theta s\psi)^2\sigma_{\dot{U}}^2 + (c\varphi s\theta s\psi - c\psi s\theta)^2\sigma_{\dot{V}}^2 + (c\varphi c\theta)^2\sigma_{\dot{W}}^2$$

The GNSS velocity variances for various flight profiles are obtained from Ding and Wang (2011). Detailed specifications for the GRS-77 AHRS used in the Garmin G1000 is undisclosed proprietary information, however typical commercial AHRS accuracy indicates an accuracy on the scale of tenths of a degree, with low drift rates due to fusion with other data sources (Northrop Grumman 2012). For the currently presented uncertainty analysis, a standard deviation of 0.5˚ for each attitude is assumed to be safely exceeding that of the Garmin system. Attitude sensors, typically Micro-Electromechanical Sensors (MEMS) Inertial Measurement Units (IMU), are subject to drift errors which decrease in magnitude with an increase in quality. The data from MEMS-IMU that are installed within an AHRS are typically processed with inputs from other flight parameters with the help of various filters to minimise the signal noise and measurement errors. Assuming these uncertainty figures for raw measurements for GNSS and MEMS-IMU and adopting Eqs. 13-15, it is possible to calculate the standard deviations related to our variables of interest (*i.e.*, the acceleration components in body axes) for various flight phases, which are listed in Table 1. The calculated standard deviations indicate that the model has the largest uncertainty when flying at increasing attitude angles. This is intuitive as in these flight conditions the aircraft orientation and velocities can vary greatly between the different reference frames. Overall, the vertical acceleration appears to have the lowest uncertainty. Large uncertainties in the computed CG accelerations would result in inaccurate estimations of the stress range experienced by critical components. Any reduction in the standard deviation of the input attitudes and GNSS derived velocities would reduce the resultant uncertainty in axial accelerations significantly.

**Table 1.** Uncertainty in CG accelerations by flight phase.

| Flight phase | $\sigma_{ax}$ (m/s²) | $\sigma_{ay}$ (m/s²) | $\sigma_{az}$ (m/s²) |
|---|---|---|---|
| Straight climb | 0.019 | 0.067 | 0.008 |
| Left turning climb | 0.047 | 0.052 | 0.013 |
| Level left turn | 0.057 | 0.263 | 0.033 |
| Straight and level | 0.051 | 0.021 | 0.007 |
| Left turning descent | 0.046 | 0.043 | 0.015 |
| Straight descent | 0.051 | 0.021 | 0.007 |

## FLIGHT TEST DATA ANALYSIS

A total number of 460 flight log files were obtained by RMIT University Flight Training for testing the proposed model. In order to reduce the dataset to the relevant periods, the indicated airspeed parameter (Fig. 5) is used to assess the "is flying" condition for times when the airspeed is significantly greater than zero for more than 30 seconds. The filtered data is processed with the presented model to determine axial loadings at the centre of gravity for each flight, and the results aggregated. A comparison with the vertical loading recorded by the G1000 is performed to support an initial validation of the model.

In a relatively small number of instances, the flight data for the flight phase was not accurate, and occasionally displayed large spikes of short duration in the velocity values, as shown in Fig. 6.

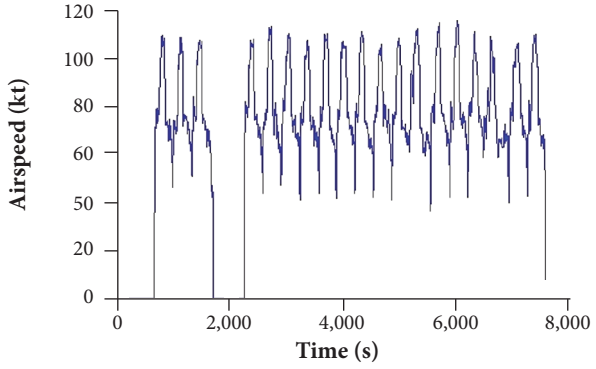


**Figure 5.** Indicated airspeed as retrieved from the log files.

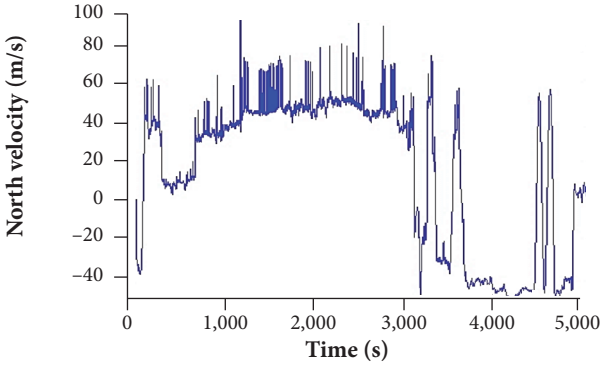


**Figure 6.** Detail of the velocity value of a flight phase displaying spikes.

These spikes were likely induced by Global Navigation Satellite Systems (GNSS) signal degradations or losses. There are various different causes for data degradation and signal losses in GNSS measurements (Sabatini *et al.* 2013b), including:

- Antenna obscuration during manoeuvres;
- Adverse satellite geometry resulting in high position dilution of precision;
- Doppler shift;
- Multipath effects;
- Interference and jamming.

Further compound analysis of the aircraft state may enable the determination of the specific causes if required. The adoption of multi-sensor architectures for accurate navigation such as the one presented in section 5 for UA can significantly contribute in mitigating similar data outages. Further data filtering by the adoption of a custom rejection criterion is required to flag log files for manual review of their validity. The criterion upon which a data rejection algorithm is implemented is as follows. For each geodetic position recorded in the data files, a check is performed to identify periods for which the acceleration incurred a reversal of magnitude greater than 10 m/s$^2$ (*i.e.*, approximately 1*g*) within 3 seconds. Files with frequent spiking in the calculated velocity are removed from the dataset and flagged for manual review. The complete data rejection algorithm is depicted in Fig. 7.

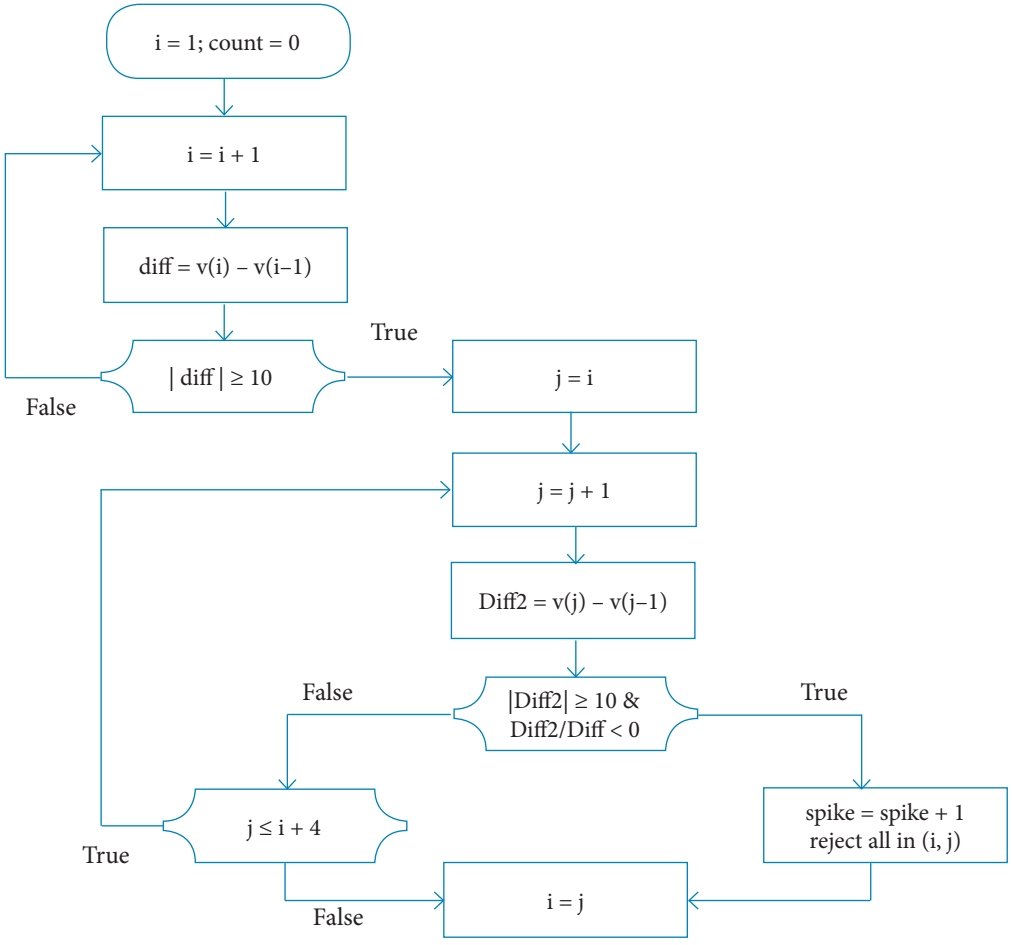


**Figure 7.** Data rejection algorithm.

A total of 280 hours of flight data were processed through the described model to generate the dynamic loads. Figure 8 compares the spectra of the vertical load calculated from the geodetic data recorded by the Garmin G1000 and manipulated by the 6-DOF based model, and the vertical load recorded by the Garmin G1000 itself. In Fig. 8 the positive loadings are defined as upwards towards the sky, and negative loadings as downwards towards the Earth. The load factor distributions are neither normally-distributed nor symmetric. This is to be expected as significant portions of the flights are conducted in horizontal steady flight conditions, and as manoeuvres at positive pitch rates occur more frequently than the ones at negative pitch rates. The 6-DOF model and the recorded load factor have a correlation coefficient of $r = 0.688\ g$, indicating an acceptable correlation between the two. The mean of the error is $\mu = 0.02\ g$ with a standard deviation $\sigma = 0.080\ g$, therefore adopting 6-DOF dynamics to retrieve dynamic loads of the aircraft from tabulated position, velocity and attitude data proves adequately accurate. The uncertainty analysis predicted greater discrepancies in the computed loads for greater loadings, and this is evident in the graph. In particular, the model shows larger positive vertical loads and smaller negative loads compared to the ones logged by the Garmin system. Although the Garmin G1000 is fitted with an AHRS equipped with accelerometers, the acceleration values logged are of uncertain origin and may not necessarily be raw measurement data and instead involve filtering and integration with other sensors. Figure 9 shows the loading spectra recalculated in the longitudinal and lateral body axes for the Cessna. The model produces accurate approximations of the loads experienced by the aircraft and can be used with an appropriate margin of safety for cumulative damage calculation.

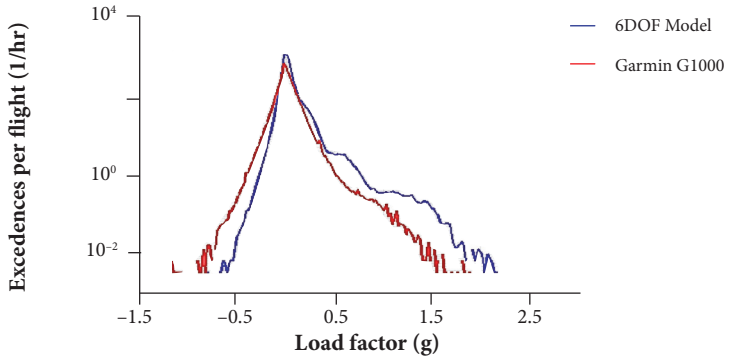


**Figure 8.** 6-DOF model-based (blue) and Garmin G1000 (red) vertical (Z) load factor spectra.

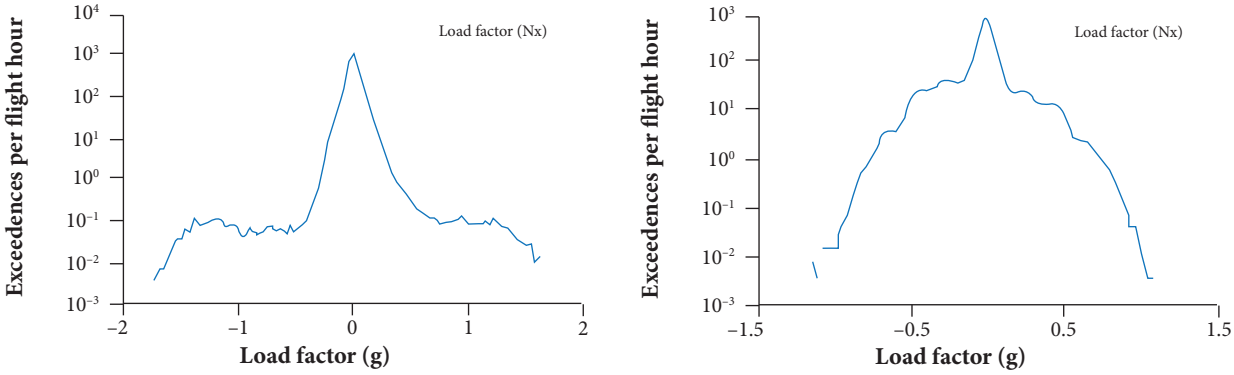


**Figure 9.** Longitudinal (X) and lateral (Y) loading factors spectra.

## FURTHER DEVELOPMENTS FOR UNMANNED AIRCRAFT

The quality of fatigue calculations performed with the proposed model is directly dependent on the accuracy and precision of the sensors used. GNSS receivers typically fitted to UA can yield good accuracy and precision for low-cost units under optimal

conditions. UA are not usually fitted with high-quality IMU due to the prohibitive cost and/or size. Instead, lower cost MEMS units are fitted, which have drift errors of larger orders of magnitude (Sabatini *et al.* 2015). Over the course of an extended flight this results in a large drift from the true value which becomes more significant the longer the flight. Using the data from such sensors would not be suitable for application with the proposed model. If the data from the GNSS and an example low-cost MEMS-IMU can be filtered and combined, large improvements to the accuracy of the system can be achieved. As outlined in Sabatini *et al.* (2015), three navigation systems can be combined to enhance the accuracy of position, velocity, attitude and accelerations measurements. The architecture illustrated in Figure 10 involves combining a Vision-Based Navigation (VBN) state, an IMU state, a GNSS states and an Aircraft Dynamic Model (ADM) state through an Extended Kalman Filter (EKF); referred to as VBN-IMU-GNSS-ADM (VIGA). The data fusion logics compares the states determined by each module and inputs them to the EKF which in turn estimates the Position, Velocity and Attitude (PVA) error which are used to adjust the IMU measurements. The corrected states are fed back into the navigation processor and ADM.

The VBN system involves the use of optical sensors (visible or infrared spectrum) to identify landscape and (generally) runway features for use in attitude determination. An Appearance Based Approach (ABA) is adopted, which involves manually guiding the aircraft through the environment to obtain key reference points. After the aircraft has been made aware of the environment, it finds the best match between an observation and a stored picture to obtain an orientation. This system is entirely reliant on the ability to identify the relevant environmental aspects (horizon, runway centreline) in the frame which is impacted by the field of view of the camera and camera quality. The performance is degraded by fog, low-light conditions, rain, etc. which affect aspect visibility. Therefore, a VBN is most useful during take-off and approach flight phases. The ADM is essentially a virtual sensor providing navigation state estimates based on the aircraft's flight dynamics. The ADM can be based on a 6-DOF flight dynamics model or on a 3-DOF flight dynamics model with appropriate considerations regarding flight phase. It is necessary for the ADM to be frequently reinitialized (~ every 20 seconds) due to the compounding nature of errors inherent to the process (Sabatini *et al.* 2013a; Sabatini *et al.* 2015). The resulting state can improve attitude determination significantly, which will then allow the proposed SHM model to determine axial loadings. As detailed in (Sabatini *et al.* 2015), the architecture is applied to an AEROSONDE UA which performed the same flight manoeuvres considered in the Cessna 172S flight test. The ADM used for the AEROSONDE as part of the VIGA integration was a 3-DOF model, not a full 6-DOF, but it is tailored to the appropriate flight phases so it is still of a high level of accuracy. The standard deviations of the errors for these flight regimes, and subsequent estimated uncertainty if the model is applied to the AEROSONDE, are given in Table 2. Although not as accurate as when applied to the Cessna, the accuracy of the model would still be sufficient to derive meaningful loading data for a structural health assessment.

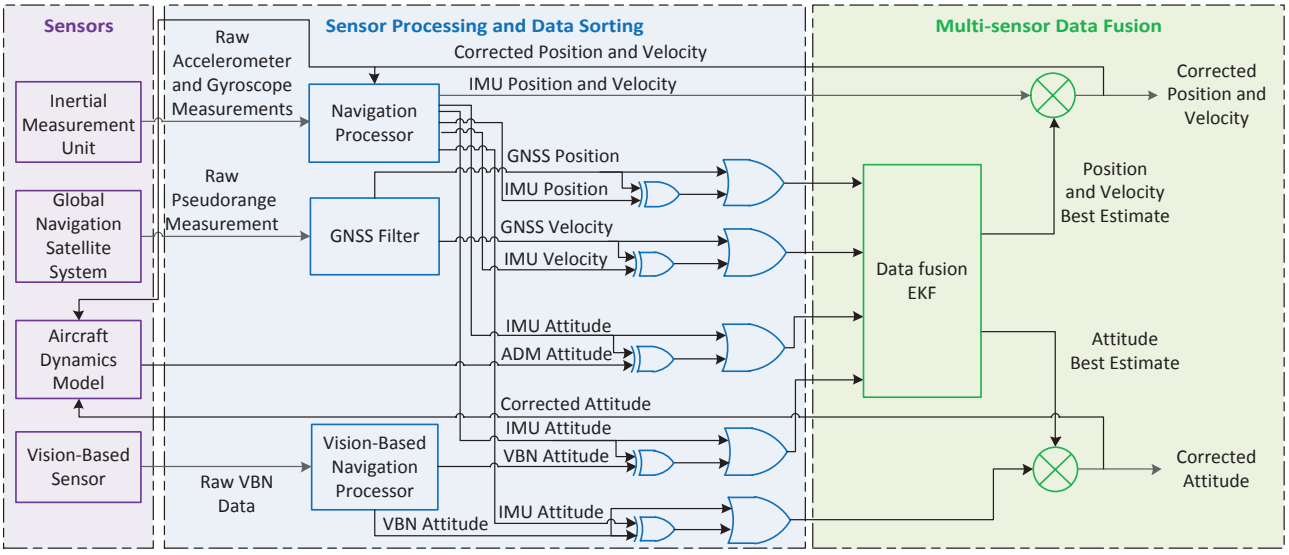


**Figure 10.** VIGA architecture. Adapted from Sabatini et al. (2013a) and Sabatini et al. (2015).

**Table 2.** VIGA error statistics and model uncertainty for AEROSONDE UA.

| Flight manoeuvre | North velocity | East velocity | Down velocity | Pitch (theta) | Roll (phi) | Yaw (psi) | $\sigma_{ax}$ (m/s²) | $\sigma_{ay}$ (m/s²) | $\sigma_{az}$ (m/s²) |
|---|---|---|---|---|---|---|---|---|---|
| Straight climb | 0.060 | 0.100 | 0.084 | 0.004 | 0.004 | 0.008 | 0.121 | 0.298 | 0.086 |
| Left-turning climb | 0.059 | 0.035 | 0.042 | 0.046 | 0.003 | 0.016 | 0.162 | 0.111 | 0.042 |
| Level left turn | 0.042 | 0.043 | 0.003 | 0.001 | 0.013 | 0.001 | 0.187 | 0.041 | 0.023 |
| Straight and level | 0.031 | 0.035 | 0.001 | 0.004 | 0.004 | 0.011 | 0.176 | 0.070 | 0.002 |
| Left-turning descent | 0.090 | 0.080 | 0.036 | 0.007 | 0.004 | 0.009 | 0.194 | 0.200 | 0.033 |
| Straight descent | 0.070 | 0.167 | 0.015 | 0.004 | 0.003 | 0.010 | 0.383 | 0.154 | 0.017 |

## CONCLUSIONS AND FUTURE WORK

A new method for assessing cumulative structural damage in General Aviation (GA) aircraft and Unmanned Aircraft (UA) exploiting flight data recorded by on-board avionics and/or from low-cost commercial-of-the-shelf navigation and guidance systems was proposed in this article. This method enables the development of cost-effective Structural Health Monitoring (SHM) solutions that meet the market demands of the Australian GA community and other countries with considerable mean fleet age, as well as of UA operators. The method processes flight data from the log files to determine the axial loads at the Centre of Gravity (CG) as a function of geodetic coordinates and Euler attitude angles. The fatigue-critical locations in the primary structure of the aircraft are identified by means of either engineering analysis or information in the Supplementary Inspection Documents (SID) of the aircraft. A rainflow stress cycle counting method is adopted to deconstruct random variable amplitude loadings. The flight data files recorded by a fleet of Cessna 172 Skyhawk aircraft equipped with Garmin G1000 digital avionics operated by RMIT University Flight Training from the Royal Australian Air Force (RAAF) Williams airbase in Point Cook (Victoria) are used for initial model verification. A quality verification and data filtering/rejection algorithm is implemented to filter-out ground manoeuvring phases as well as data spikes resulting from navigation signal degradations or losses. An uncertainty analysis was performed to determine the estimated error figures of the SHM system in various flight phases and consequently assess the overall accuracies. The values for vertical acceleration derived from the model are also compared to the recorded ones to evaluate the model accuracy. Future flight test activities will involve the assessment of cumulative fatigue damage on critical structural components on a test bed aircraft fitted with suitable flight test instrumentation (*e.g.*, strain gauges) to experimentally validate the model correlation parameters. The model will also be extended to include multiaxial fatigue analysis. Different counting methods that have been explored in the literature will be investigated in future research (Weber *et al.* 1999; Koski *et al.* 2006).

## AUTHOR'S CONTRIBUTION

Conceptualization, Keryk C, Sabatini R and Kourousis K; Methodology, Keryk C, Sabatini R, Kourousis K, and Silva J; Investigation, Keryk C, Sabatini R, Gardi A and Silva J; Writing – Original Draft, Keryk C, Sabatini R, Gardi A and Silva J; Writing – Review & Editing: Gardi A, Silva J and Sabatini R.

# REFERENCES


Aktepe B, Molent l (1999) Management of airframe fatigue through individual aircraft loads monitoring programs. Proceedings of International Aerospace Congress; Adelaide, Australia.

Boller C, Buderath M (2007) Fatigue in aerostructures – where structural health monitoring can contribute to a complex subject. Philosophical transactions of the Royal Society Series A: Mathematical, physical, and engineering sciences 365(1851):561-587. doi: 10.1098/rsta.2006.1924

Cicero JA, Feiter FL, Mohammadi J (2001) Statistical loads data for Cessna 172 aircraft using the Aircraft Cumulative Fatigue System (ACFS). DOT/FAA Report AR-01/044.

Civil Aviation Safety Authority (2012) Take a closer look – The ageing aircraft resource. SP135.

Ding W, Wang J (2011) Precise velocity estimation with a stand-alone GPS receiver. Journal of Navigation 64(2):311-325. doi: 10.1017/s0373463310000482

Dowling NE (1988) Estimation and correlation of fatigue lives for random loading. International Journal of Fatigue 10(3):179-185. doi: 10.1016/0142-1123(88)90060-6

Federal Aviation Authority (2005) Fatigue, fail-safe, and damage tolerance evaluation of metallic structure for normal, utility, acrobatic, and commuter category airplanes. FAA Advisory Circular AC23-13A.

Iyyer N, Sarkar S, Merrill R, Bradfield S (2008) Management of aging aircraft using deterministic and probabilistic metrics. Proceedings of 11th Joint NASA/FAA/DOD Conference on Aging Aircraft; Phoenix, AZ, USA.

Koski K, Tikka J, Backstrom M, Siljander A, Liukkonen S, Marquis G (2006) An aging aircraft's wing under complex multiaxial spectrum loading: Fatigue assessment and repairing. International Journal of Fatigue 28(5-6):652-656.

Kourousis KI (2013) A holistic approach to general aviation aircraft structural failure prevention in Australia. Aviation 17(3):98-103. doi: 10.3846/16487788.2013.840055

Marczi T, Ruzicka M, Slavik S (2004) Fatigue monitoring and operational safety improvement of small sport planes. Proceedings of 24th International Congress of the Aeronautical Sciences (ICAS 2004); Yokohama, Japan.

Marczi T (2004) Acceleration fatigue of small airplanes – Measurement, evaluation and fatigue life prediction (PhD thesis). Prague, Czech Republic: Czech Technical University.

McColl C, Iyyer N (2008) A template for successful development and implementation of an aircraft life tracking program. Proceedings of 11th Joint NASA/FAA/DOD Conference on Aging Aircraft; Phoenix, AZ, USA.

Molent L, Aktepe B (2000) Review of fatigue monitoring of agile military aircraft. Fatigue & Fracture of Engineering Materials & Structures. 23:767-785. doi: 10.1046/j.1460-2695.2000.00330.x

Molent L, McDonald M, Barter S, Jones R (2008) Evaluation of spectrum fatigue crack growth using variable amplitude data. International Journal of Fatigue 30(1):119-137. doi: 10.1016/j.ijfatigue.2007.02.025

Musallam M, Johnson CM (2012) An efficient implementation of the rainflow counting algorithm for life consumption estimation. IEEE Transactions on Reliability 61(4):978-986. doi: 10.1109/tr.2012.2221040

Northrop Grumman (2012) LCR-100 Gyrocompass AHRS Technical Data; [accessed 2017 Oct. 11]. http://www.northropgrumman.litef.com/fileadmin/downloads/Datenblaetter/Datenblatt_LCR-100.pdf

Ocampo JD, Millwater HR, Smith H, Meyer E, Nuss M, Reyer M, Abali F, Shiao M (2010) Probabilistic risk assessment for small airplanes. Proceedings of 51st AIAA/ASME/ASCE/AHS/ASC Structures, Structural Dynamics, and Materials Conference; Orlando, FL, USA. doi: 10.2514/6.2010-2680

Olkiewicz C, Mohammadi J, Cicero J (1994) Design, manufacture, and test of a flight load recorder for small aircraft. DOT/FAA Technical Note CT-TN93/23.

Sabatini R, Cappello F, Ramasamy S, Gardi A, Clothier R (2015) An innovative navigation and guidance system for small unmanned aircraft using low-cost sensors, in press, Aircraft Engineering and Aerospace Technology. doi: 10.1108/aeat-06-2014-0081

Sabatini R, Moore T, Hill C (2013a) A new avionics-based GNSS integrity augmentation system: Part 1 – Fundamentals. Journal of Navigation 66:363-384. doi: 10.1017/s0373463313000027

Sabatini R, Ramasamy S, Gardi A, Rodriguez Salazar L (2013b) Low-cost sensors data fusion for small size unmanned aerial vehicles navigation and guidance. International Journal of Unmanned Systems Engineering 1:16-47. doi: 10.14323/ijuseng.2013.11

Swanton G, Walker K (1997) Development of transfer functions to relate F-111 Aircraft Fatigue Data Analysis System (AFDAS) strain outputs to loads and control point stresses. Defence Science and Technology Organisation (DSTO) Technical Report 0463/AR-010-278, Australian Department of Defence.

Wahab MS, Paramonov YM (2010) The influence of corrosion on reliability and inspection program for fatigue-prone airframe structures. Aviation 8(3):37-41.

Weber B, Carmet A, Kenmeugne B, Robert JL (1999) A stress-based approach for fatigue assessment under multiaxial variable amplitude loading. European Structural Integrity Society 25:218-231. doi: 10.1016/s1566-1369(99)80017-x

Xiang Y, Liu Y (2011) Application of inverse first-order reliability method for probabilistic fatigue life prediction. Probabilistic Engineering Mechanics 26(2):148-156. doi: 10.1016/j.probengmech.2010.11.001

Zeiler TA, Tipps DO, Skinn DA, Rustenburg JW (2001) Preliminary results of BE-1900D operational flight loads data evaluation. AIAA Journal of Aircraft 38(3):565-572. doi: 10.2514/2.2799

Zhuang W, Barter S, Molent L (2007) Flight-by-flight fatigue crack growth life assessment. International Journal of Fatigue 29(9-11):1647-1657. doi: 10.1016/j.ijfatigue.2007.01.029

Zipfel PH (2007) Modeling and simulation of aerospace vehicle dynamics. 2nd ed. Reston, VA, USA: American Institute of Aeronautics and Astronautics (AIAA): 2007. doi: 10.1017/s0001924000087984